

D-Lite: Navigation-Oriented Compression of 3D Scene Graphs under Communication Constraints

Yun Chang^{1,*}, Luca Ballotta^{2,*}, Luca Carlone¹

Abstract—For a multi-robot team that collaboratively explores an unknown environment, it is of vital importance that collected information is efficiently shared among robots in order to support exploration and navigation tasks. Practical constraints of wireless channels, such as limited bandwidth and bit-rate, urge robots to carefully select information to be transmitted. In this paper, we consider the case where environmental information is modeled using a *3D Scene Graph*, a hierarchical model that describes geometric and semantic aspects of the environment. Then, we leverage graph-theoretic tools, namely *graph spanners*, to design heuristic strategies that efficiently compress 3D Scene Graphs to enable communication under bandwidth constraints. Our compression strategies are *navigation-oriented* in that they are designed to approximately preserve shortest paths between locations of interest, while meeting a user-specified communication budget constraint. Effectiveness of the proposed algorithms is demonstrated via extensive numerical analysis and on synthetic experiments in a realistic simulator.

I. INTRODUCTION

In the near future, robot teams will perform coordinated and cooperative tasks in various application scenarios, ranging from exploration of subterranean environments, to search-and-rescue missions in hazardous settings, to human assistance in houses, airports, factory floors, and malls, to mention a few.

A key requirement for coordinated exploration and navigation in an initially unknown environment is to build a map model of the environment as the robots explore it. Recent work has proposed *3D Scene Graphs* as an expressive hierarchical model of complex environments [1–4]: a 3D Scene Graph organizes spatial and semantic information, including objects, structures (e.g., walls), places (i.e., free-space locations the robot can reach), rooms, and buildings into a graph with multiple layers corresponding to different levels of abstraction. 3D Scene Graphs provide a user-friendly model of the scene that can support high-level instructions by a human, for instance allowing a person to ask a robot to bring her a cup of coffee rather than providing Euclidean coordinates of the cup.

Scaling up from single-robot to multi-robot systems, a key challenge is to share the map information among the robots in the team to support coordination. For instance, the robots may exchange partial maps such that a robot can more efficiently

navigate within a portion of the environment mapped by another robot. However, the potentially high volume of data to be transferred over a shared wireless channel can easily saturate the available bandwidth, degrading team performance. This is particularly relevant when the map is model as a 3D Scene Graph, since these are rich and potentially large models if all the nodes and layers are retained. On the other hand, 3D Scene Graphs also provide opportunities to compress information: for instance, the robots may exchange information about rooms in the environment rather than sharing fine-grained traversability information encoded by the places layer; similarly, for a large-scale scene, the robot may just specify a sequence of buildings to be traversed, abstracting away low-level geometric information. This is not dissimilar from what humans do: when providing instructions to another person about how to navigate to a location in a building, we would specify a sequence of rooms and landmarks (e.g., objects or structures) rather than communicating a detailed metric map.

Therefore, the question we address in this paper is: *how can we compress a 3D Scene Graph to retain relevant information the robots can use for navigation, while meeting a communication budget constraint, expressed as the maximum size of the map the robots can transmit?* Besides multi-robot communication, task-driven map compression may also play a key role in long-term autonomy of resource-constrained robots, where the robots might be unable to store very large-scale maps due to memory constraints.

Related work. Graph compression has been an active area of research in discrete mathematics, computer science, and telecommunications, where it finds applications to vehicle routing [5], packet routing in wireless networks [6], or compression of unstructured data such as 3D point clouds [7].

A prominent body of works aims to simplify an input graph by carefully removing edges based on structural properties of the graph. This kind of methods typically entail some information loss, and aim to only retain relevant information. For example, references [6, 8] find efficient representations of huge web and communication networks by heuristically selecting a few key graph elements, while the work [9] compresses graphs while preserving connectivity among nodes. Within the mathematical literature, graph compression has been studied with attention to ensuring low distortion of inter-node distances. For example, *spanning trees* and *Steiner trees* are the smallest subgraphs ensuring connectivity in undirected graphs [10, 11]. Conversely, *graph spanners* aim to remove edges while allowing for a user-defined maximum distortion of shortest paths [12]. A special case of the latter are *distance preservers* [13], that prune graphs but also keep shortest

This work was partially funded by ARL DCIST CRA W911NF-17-2-0181, ONR RAIDER N00014-18-1-2828, Lincoln Laboratory’s Resilient Perception in Degraded Environments program, the CARIPARO Foundation Visiting Programme “HiPeR”, and the Italian Ministry of Education under the initiative “Departments of Excellence” (Law 232/2016).

¹Laboratory for Information & Decision Systems (LIDS), Massachusetts Institute of Technology, Cambridge, MA, USA, {yunchang, lcarlone}@mit.edu.

²Department of Information Engineering, University of Padova, Padova, Italy, ballotta@dei.unipd.it.

*Equal contribution.

paths for specified node pairs. Conversely, *emulators* allow for replacing a large number of edges with a few strategic ones to ensure small stretch of distances among nodes [14].

On the other hand, lossless compression strategies aim to find compact representations of graphs to be efficiently stored or processed. A subset of related work directly deals with communication-efficient re-labeling of nodes that enhance graph encoding. For example, some classical methods exploit algebraic tools such as spectral decomposition of the incidence or adjacency matrix that allow encoding the latter with a limited number of codewords, while paper [15] proposes an algorithm that exploits graph structures such as hubs and spokes. A recent survey of lossless compression techniques is given in [16]. A different paradigm for lossless compression is based on hypergraphs, which generalize standard graphs by allowing hyperedges that connect more than two nodes. Among others, paper [17] tailors semantic data compression, [18] proposes a procedure to construct hypergraphs from network data, [19, 20] tackle hypergraph partitioning, and [21] presents a signal processing framework based on hypergraphs.

Related work in robotics has put more emphasis on graph compression to speed up path planning and decision-making algorithms. For instance, Silver *et al.* [22] exploit Graph Neural Networks to detect key nodes by learning heuristic importance scores. Agia *et al.* [23] propose an algorithm that exploits the 3D Scene Graph hierarchy to prune nodes and edges not relevant to the robotic task. Targeting a related application domain, Tian *et al.* [24] study computation and communication efficiency of multi-robot loop closure, providing a strategy to share a limited number of visual features in multi-robot visual SLAM. Finally, the line of work [25–27] proposes algorithms to derive hierarchical abstractions of tree-structured representations, for instance enabling fast planning on occupancy grid maps at progressively increasing resolution.

Novel contribution. In this paper, we tackle the challenging problem of efficiently sharing 3D Scene Graphs for navigation tasks under communication constraints. Differently from existing literature, we propose novel compression algorithms that crucially exploit on the one hand navigation-related information, and on the other hand both spatial information and hierarchical structure of the 3D Scene Graph. Our algorithms are computationally efficient and apply to general graphs. In contrast, closely related works are either restricted to trees or involve mixed-integer programming [25, 26]. Further, we allow for loose specification of navigation tasks to make our approach flexible to inexact or uncertain queries, that may reflect lack of knowledge about an unexplored portion of the environment that a querying robot needs to traverse, while other work targets single-task compression with focus on computational efficiency of local planning algorithms [23]. Also, we ground our algorithms in a preexisting semantic hierarchy, and incorporate task-relevant spatial information in the compression procedure. In contrast, the approach in [25] builds geometric abstractions on-the-fly and does not exploit semantic or hierarchical information of the graph to be compressed. To meet a sharp budget on transmitted information,

we design suitable heuristics that exploit graph spanners of the 3D Scene Graph to be sent: these mathematical tools allow to trade size of a subgraph of the 3D Scene Graph to be compressed for the maximum distortion suffered by shortest paths between nodes. The latter feature helps us design compression algorithms with attention to navigation tasks, for which paths planned on the compressed graph are not much longer compared to planning on the original graph with fine-scale spatial information. In contrast, other works addressing real-time compression do not allow for hard communication constraints, either turning to soft constraints in the form of Lagrangian-like regularization [25], or focusing on computational aspects with feasibility requirements [23]. In particular, the latter work simply proposes to prune the 3D Scene Graph to boost efficiency of a path planning routine, but it does not allow for sharp bounds on the size of the pruned graph, and further assumes that a specific task is known beforehand and only needs to be efficiently planned by the robot (*e.g.*, finding an efficient way to grab and move specified objects).

Effectiveness of our algorithms is validated through realistic simulation experiments that illustrate how our proposed methods provide satisfaction of hard communication constraints without excessively impacting efficiency of navigation tasks. For example, we show that navigation time on the compressed graph increases at most by as little as 8% while retaining only 1.6% of the full 3D Scene Graph.

Paper organization. In Section II, we present the motivating setup for navigation-oriented compression in the presence of communication constraints, and state the 3D Scene Graph compression as an optimization problem which can be exactly solved by an Integer Linear Program (ILP). To circumvent computational intractability of the ILP in practice, we design efficient algorithms that ensure to meet available communication resources while retaining spatial information useful for navigation. In particular, we leverage graph spanners to trade size of the compressed graph for distortion of shortest paths: mathematical background on spanners is provided in Section III, while explanation of our proposed algorithms is detailed in Section IV. In Section V, we test our approach with realistic simulation software for robotic exploration, and compare it to the compression approach in [25]. Final remarks and future research directions are given in Section VI.

II. NAVIGATION-ORIENTED DSG COMPRESSION

Motivating scenario. We consider a multi-robot team exploring an unknown environment. Each robot navigates to gather information and builds a 3D Scene Graph (DSG) $\mathcal{G} = (\mathcal{V}_{\mathcal{G}}, \mathcal{E}_{\mathcal{G}})$ that describes the portion of the environment explored so far [3, 28, 29]. As robots are scattered across a possibly large area, they exchange information to cooperatively gather information about the environment. In particular, a robot r_1 may query another robot r_2 to get information about the area

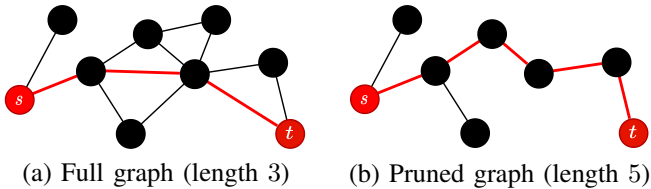


Figure 1: Distortion of shortest path from s to t (thick red).

explored by r_2 but still unknown to r_1 .¹

Navigation-oriented query. In this paper, we assume that the querying robot r_1 needs to reach one or more *target locations* $\mathcal{T} \subset \mathcal{V}_{\mathcal{G}}$ within the DSG $\mathcal{G} = (\mathcal{V}_{\mathcal{G}}, \mathcal{E}_{\mathcal{G}})$ of robot r_2 . Such locations, for instance, may be objects of interest or points of interest (*e.g.*, the building exits). Hence, r_2 shall transmit (a portion of) its local map such that r_1 can reach locations in \mathcal{T} from a set $\mathcal{S} \subset \mathcal{V}_{\mathcal{G}} \setminus \mathcal{T}$ of *source locations*. In practice, the latter may correspond to physical access points (*e.g.*, doors) to the area explored by r_2 that are close to the current location of r_1 , and may be either communicated by r_1 or estimated by r_2 based on r_1 's position. In the following, we generically refer to sources and targets as *terminals*, which for the sake of this work are assumed to be *places* nodes in the DSG.

Communication constraints. Data sharing among robots occurs over a common wireless channel. Because of resource constraints of wireless communication, such as limited bit-rate and bandwidth, robot r_2 cannot transmit its entire DSG to robot r_1 . Specifically, we assume that robots can only send a small portion of their DSG each time they receive a share request.² Hence, queried robot r_2 needs to compress its DSG \mathcal{G} into a smaller graph $\mathcal{G}' = (\mathcal{V}_{\mathcal{G}'}, \mathcal{E}_{\mathcal{G}'})$, with at most B nodes (where B reflects the available communication budget), that complies with communication constraints while retaining information useful for robot r_1 to navigate between the terminal nodes.

Pruning 3D Scene Graph. Assuming navigation-oriented queries, the relevant information reduces to nodes and edges enabling efficient paths robot r_1 can use to move from sources to targets. Specifically, the collection of all shortest paths between each source $s \in \mathcal{S}$ and target $t \in \mathcal{T}$ represents the minimal information that can be transmitted to ensure that navigation by r_1 takes the minimum possible time, *i.e.*, the time a robot with complete knowledge of the map would take.

However, transmitting all nodes in the shortest paths may violate the communication constraint: this can happen with many terminals or if shortest paths have little overlap. Hence, heavier pruning of the DSG might be needed to make communication feasible. This means that information useful for path planning will be partially unavailable to querying robot's planner. In other words, because the DSG \mathcal{G} cannot be fully

¹We assume robots talk with each other as soon as they get within communication range.

²Communication constraints can be practically intended as maximum transmission time T_{\max} : a robot first senses the channel and then, based on available communication resources, estimates the amount of information that can be sent in time T_{\max} . For example, assuming bit-rate r , specification of T_{\max} unambiguously defines the maximum amount of bits $b_{\max} = rT_{\max}$ to be sent, which is mapped to a DSG-related quantity (*e.g.*, number of nodes).

communicated, the distance (length of a shortest path) between a pair of terminals in the transmitted graph \mathcal{G}' will be larger than the distance between those same terminals in the original DSG. A schematic example is provided in Fig. 1, where the length of the shortest path between nodes s and t increases from 3 to 5 after node and edge removal. For example, a robot may prune place nodes within a room, or share only the room node as a coarse representation of places. This requires less communication, but the querying robot r_1 , which receives a coarse-scale map, will be forced to, *e.g.*, taking a longer detour across a room, instead of traversing the original shortest path along a set of places nodes. Mathematically, this is expressed as $d_{\mathcal{G}'}(s, t) \geq d_{\mathcal{G}}(s, t)$ for any $s \in \mathcal{S}$ and for any $t \in \mathcal{T}$, where $d_{\mathcal{G}}(u, v)$ is the distance from node u to node v in graph \mathcal{G} .

Problem formulation. For the querying robot r_1 to navigate efficiently, it is desirable that the distance $d_{\mathcal{G}'}(s, t)$ between s and t in the transmitted graph \mathcal{G}' is not much larger than the distance in the original graph \mathcal{G} . Hence, the transmitting robot shall select nodes and edges in \mathcal{G}' so as to minimize the *distortion*, or *stretch*, between shortest paths in the original and compressed graphs. This can be cast into the following optimization problem,

$$\begin{aligned} \min_{\mathcal{G}' \subseteq \mathcal{G}} \quad & \beta & (1a) \\ \text{s.t.} \quad & d_{\mathcal{G}'}(s, t) \leq d_{\mathcal{G}}(s, t) + \beta W_{\max}^{\mathcal{G}}(s, t) \quad \forall (s, t) \in \mathcal{P}, & (1b) \\ & |\mathcal{V}_{\mathcal{G}'}| \leq B, & (1c) \end{aligned}$$

where $W_{\max}^{\mathcal{G}}(u, v)$ denotes the maximum edge weight on a shortest path from u to v in \mathcal{G} , and $\mathcal{P} \subseteq \mathcal{S} \times \mathcal{T}$ is the set of source-target pairs considered for compression. Constraint (1c) ensures that the amount of transmitted information (number of nodes) meets communication constraint, while constraint (1b) and cost (1a) encode minimization of the maximum distortion incurred by the shortest paths. The multiplicative coefficient $W_{\max}^{\mathcal{G}}(s, t)$ in (1b) is necessary to make the distortion computation meaningful for weighted graphs.

Problem (1) can be solved exactly by means of integer linear programming (ILP), see Appendix A. However, the runtime complexity of ILP solvers is subject to combinatorial explosion, making this approach impractical for online operation. Hence, we propose greedy algorithms that require lighter-weight computation, based on *graph spanners*.

III. BACKGROUND: GRAPH SPANNERS

We ground our compression algorithm in the concept of *graph spanner* [12]. In words, a spanner is a compressed (*i.e.*, sparse) representation of a graph such that shortest paths between nodes are distorted at most by a user-defined stretch. Formally, spanner $\mathcal{G}' = (\mathcal{V}, \mathcal{E}')$ of graph $\mathcal{G} = (\mathcal{V}, \mathcal{E})$ is a subgraph such that $\mathcal{E}' \subseteq \mathcal{E}$ and the following inequality holds for $u, v \in \mathcal{V}$,

$$d_{\mathcal{G}'}(u, v) \leq \alpha d_{\mathcal{G}}(u, v) + \beta W_{\max}^{\mathcal{G}}(u, v), \quad (2)$$

where $\alpha \geq 1$ and $\beta \geq 0$ are given constants. For generic α and β , \mathcal{G}' is called an (α, β) -spanner, whereas if β (resp. α) is equal to zero (resp. one) it is called α -multiplicative spanner

(resp. β -additive or $+\beta$ spanner). Inequality (2) may hold for all nodes in \mathcal{G} or for a few pairs as in (1b): in the latter case, the resulting subgraph is referred to as a *pairwise spanner*.

Applications of spanners include navigation or packet routing in large graphs, whose size makes running path planning algorithms in the original graph computationally infeasible, [30, 31]. In this case, one can compute a spanner of the original graph and run planning algorithms on the spanner instead.

As one can see from (2), the characterization of spanners shares similarity with problem (1). Unfortunately, no method is known in the literature to build a spanner given a fixed node (or edge) budget, whereas algorithms usually enforce stretch (2) given input parameters α and β while attempting to minimize the total spanner edge-weight to obtain lightweight representations. The standard formulation of the graph spanner problem can be then written as follows [12, Problem 2],

$$\min_{\mathcal{E}_{\mathcal{G}'} \subseteq \mathcal{E}} \sum_{(i,j) \in \mathcal{E}_{\mathcal{G}'}} W^{\mathcal{G}}(i,j) \quad (3a)$$

$$\text{s.t.} \quad d_{\mathcal{G}'}(s,t) \leq \alpha d_{\mathcal{G}}(s,t) + \beta W_{\max}^{\mathcal{G}}(s,t), \quad (3b)$$

where $W^{\mathcal{G}}(i,j)$ is the weight of edge (i,j) and the objective function for unweighted graphs reduces to counting the number of edges. For multiplicative spanners this problem was quickly solved, with the classical work [32] proposing and analyzing a greedy algorithm which is known to be the best (in terms of spanner size) that runs in polynomial time. Additive and mixed spanners are instead more complex to build, and many algorithms have been proposed in the literature: early efforts were devoted to unweighted graphs [33–36], while subsequent work has focused on the general weighted case [37–40]. Other studies are concerned with distributed [41] and dynamical [42] methods, Euclidean graphs [43], and reachability preservation in digraphs [44], to mention a few.

To the best of our knowledge, the only paper to address the presence of an edge budget E_{\max} is [45]. However, the proposed algorithm receives in input also parameters α and β , and checks feasibility of an (α, β) -spanner with at most E_{\max} edges. Furthermore, its runtime increases exponentially with E_{\max} , making it unsuitable for robotics applications.

A possible way to tackle the problem at hand is to iteratively build spanners with larger and larger distortion, until the budget is met. However, several issues can hamper such a strategy. First, running a spanner-building algorithm several times may be time-consuming. Second, while small-sized (*i.e.*, with $O(n^{1+\varepsilon(\alpha)})$ edges, for some $\varepsilon(\alpha) > 0$) multiplicative spanners can be built for any given constant coefficient $\alpha \geq 1$, few constant-distortion additive spanners are known for weighted graphs, with coefficient $\beta \in \{2, 4, 6\}$. Conversely, *polynomial* distortion $\beta = \beta(n)$ is needed to build additive spanners with near-linear size [35], thus the trade-off between spanner sparsity and path distortion is not easy to exploit.

An important point is that multiplicative and additive distortion may yield dramatic differences in paths induced by the spanner. In particular, multiplying path length by a constant factor in large graphs may be undesirable in practice:

for example, if a navigation task nominally takes one hour, stretching it to two or three hours yields substantial performance degradation. Conversely, additive stretch is usually preferred because it provides a constant time overhead, which is why we used this kind of distortion in our problem formulation.

In the following, we illustrate a heuristic procedure that allows us to meet the budget constraint in (1c), runs in real time, and enforces a low distortion of shortest paths as measured by condition (1b).

IV. 3D SCENE GRAPH COMPRESSION ALGORITHMS

We propose D-Lite, a compression method for DSGs to meet communication constraints with attention to navigation efficiency. D-Lite comes in two versions, which leverage a spanner of the original full DSG (Section IV-B) and tackle the compression problem from opposite perspectives.

The first algorithm, BUD-Lite (Section IV-C), performs progressive bottom-up compression of the computed spanner, exploiting the DSG abstraction hierarchy. In contrast, the second algorithm, TOD-Lite, (Section IV-D), works top-down expanding nodes with the spanner as a target.

A. The Role of the 3D Scene Graph Hierarchy

Ideally, navigation-oriented compression of a DSG would require evaluating all possible node-pruning options to minimally stretch paths between terminal pairs. Such a search is subject to combinatorial blow-up and is not feasible in practice. Hence, we seek a greedy procedure that removes spatial information contained in the DSG while trying to limit the incurred path stretch. This goal is subject to a nontrivial trade-off. On the one hand, to ensure low stretch (enhancing navigation performance), it is desired to parse one or a few nodes at each iteration so as to introduce extra distortion in a fine-tuned, controlled way. On the other hand, parsing too few nodes at each time causes a lot of total iterations, and is time-costly for online operation. Hence, an effective algorithm should efficiently choose the size of node batch to be considered at each iteration to strike a balance between compression quality and runtime.

Towards this goal, we crucially exploit the *hierarchical structure* of the DSG. The latter allows us to see a node n_{ℓ} in layer ℓ of the DSG \mathcal{G} as a “compressed” representation of its children nodes $\mathcal{V}_{\mathcal{G}}(n_{\ell})$ in layer $\ell + 1$: hence, transmitting n_{ℓ} rather than $\mathcal{V}_{\mathcal{G}}(n_{\ell})$ saves communication while also conveying partial spatial information about $\mathcal{V}_{\mathcal{G}}(n_{\ell})$. For example, assume that $\mathcal{V}_{\mathcal{G}}(n_{\ell})$ represents a set of places within a room and n_{ℓ} is an abstraction of that room, *e.g.*, geometrically described by the coordinates of the room centroid. Then, if a robot needs to reach a specific location in $\mathcal{V}_{\mathcal{G}}(n_{\ell})$ (*e.g.*, the exit door), it can first approach the room center n_{ℓ} and then explore the area until it finds the target. This extra exploration (corresponding to additional path stretch in the compressed DSG) will negatively impact navigation time, however it allows for great compression rate useful to meet the communication constraint. From a mathematical standpoint, the navigation time needed to explore an area (*e.g.*, to go from the room center to a place) is encoded

into weights of cross-layer edges, and similarly for edges connecting nodes in the same layer with no direct path (e.g., to move from a room to another room without knowledge of place nodes). Details about the calculation of such weights, which we assume the robot with the full DSG can estimate, are provided in Appendix B .

The discussion above suggests an iterative approach to compress the DSG: at each iteration of a greedy procedure, a node at layer ℓ can be used to replace its children nodes at layer $\ell + 1$. Every time we “abstract away” places nodes for more abstract nodes (e.g., rooms, buildings) the length of the paths passing through those nodes will increase. Therefore, we can opportunistically select places nodes that entail a small stretch in the paths between the terminal nodes. In alternative, we can start with a minimal representation (e.g., one including only rooms and buildings) and iteratively expand it to reduce the stretch of the paths between terminal nodes. We present these two greedy strategies below, and initialize both procedures by computing a spanner of the given DSG, as described below.

B. Building DSG Spanner

Both proposed algorithms built a spanner of the DSG at initialization. A detailed description of how each procedure uses this spanner is deferred to Sections IV-C and IV-D.

Algorithm 1 describes how to build a spanner of the DSG that enforces a user-defined maximum additive stretch for distances between specified terminal pairs in \mathcal{P} . We adapt our algorithm from [37, Section 5]. Specifically, the procedure [37] can trade spanner size for stretch according to input parameters, building a $+cn^{\frac{1-\epsilon}{2}}\alpha W_{\max}^{\mathcal{G}}$ spanner of size $O(n^{1+\epsilon})$.³ That algorithm is intended for generic spanners (not pairwise), hence we adapt it to our scope by retaining only nodes and edges needed to connect terminal pairs in \mathcal{P} , and deleting all others.

Algorithm 1 is composed of two sequential stages: an initialization phase that builds a temporary spanner \mathcal{G}'' with a small number of edges that attempts to keep low initial path distortions, and a “buying” phase where edges are added to meet the stretch constraint. The initialization selects edges in three ways: performing a d -light initialization [39, Section 2] with appropriate d (Line 1), which in words ensures that each node has some initial neighbors; randomly picking cross-layer edges to exploit the DSG hierarchy (Line 2); adding a greedy multiplicative spanner [32, Section 2] to reduce large path distortions (Line 3). Then, for each pair (s, t) the shortest path $P_{\mathcal{G}''}(s, t)$ from source s to target t in the temporary spanner \mathcal{G}'' is considered (in suitable order): in case the stretch in \mathcal{G}'' exceeds the constraint, edges and nodes from a shortest path in the original graph \mathcal{G} are added to both \mathcal{G}'' and the final spanner \mathcal{G}' (Lines 8–9), otherwise, the shortest path in \mathcal{G}'' is directly added to the final spanner \mathcal{G}' (Line 11).

Before diving into the core of compression algorithms, it is worth reinforcing the motivation to use spanners. Algorithm 1 computes a spanner with given maximal stretch of shortest paths, but does not guarantee the size of the spanner is smaller

Algorithm 1 Build spanner

Input: DSG \mathcal{G} , terminal pairs \mathcal{P} , user parameters $\epsilon > 0, p \in [0, 1], \alpha > 2, c > 0$.

Output: DSG spanner \mathcal{G}' .

```

1:  $\mathcal{G}'_1 \leftarrow n^\epsilon$ -light initialization of  $\mathcal{G}$ ;
2:  $\mathcal{G}'_2 \leftarrow$  random sample of cross-layer edges of  $\mathcal{G}$  w.p.  $p$ ;
3:  $\mathcal{G}'_3 \leftarrow \alpha$ -multiplicative spanner of  $\mathcal{G}$ ;
4:  $\mathcal{G}'' \leftarrow \mathcal{G}'_1 \cup \mathcal{G}'_2 \cup \mathcal{G}'_3$ ; // to compute paths
5:  $\mathcal{G}' \leftarrow \mathcal{P}$ ;
6: for each  $(s, t) \in \mathcal{P}$  do // sorted by  $W_{\max}^{\mathcal{G}}(s, t)$ 
7:   if  $d_{\mathcal{G}''}(s, t) > d_{\mathcal{G}}(s, t) + cn^{\frac{1-\epsilon}{2}}\alpha W_{\max}^{\mathcal{G}}(s, t)$  then
8:      $\mathcal{G}'' \leftarrow \mathcal{G}'' \cup P_{\mathcal{G}}(s, t)$ ;
9:      $\mathcal{G}' \leftarrow \mathcal{G}' \cup P_{\mathcal{G}}(s, t)$ ;
10:  else
11:     $\mathcal{G}' \leftarrow \mathcal{G}' \cup P_{\mathcal{G}''}(s, t)$ ;
12:  end if
13: end for
14: return  $\mathcal{G}'$ .

```

than a given size. As noted in Section III, we cannot straightly apply a state-of-the-art spanner construction because no real-time algorithm addresses the presence of a budget. However, building a spanner greatly reduces the graph to be compressed up front, retaining a fraction of nodes and edges which is both relevant to the navigation task and considerably increases the efficiency of our compression algorithms. Moreover, even though path distortion may be increased to satisfy communication requirements, the user-defined stretch guaranteed by the spanner algorithm allows us to start from a maximum desired distortion, hence, if the latter is chosen loose enough, we may expect that the spanner output by Algorithm 1 is already somehow close to the communication constraint, so that additional distortion will not be very high. In particular, the spanner construction leverages overlapping portions of paths to select a handful of key edges and nodes, whereas other navigation-efficient constructions, such as the collection of all shortest paths, do not exploit the graph structure to enhance compression. Further, there are no tight bounds for the size of shortest paths, hence one cannot predict how much paths will be stretched to meet the communication budget.

C. BUD-Lite: a Bottom-Up Compression Algorithm

The key idea behind our first algorithm (BUD-Lite, short for Bottom-Up D-Lite) is to iteratively *compress nodes* in the spanner resulting from Algorithm 1 as discussed in Section IV-A. **The core mechanism is simple: we progressively replace batches of nodes with their parents to reduce budget (e.g., removing place nodes and adding the associated room node), while keeping low the distortion suffered by shortest paths between terminals. The procedure is depicted in Fig. 2.**

Algorithm 2 initially sets the compressed graph as the DSG spanner \mathcal{G}' output by Algorithm 1 (Line 1). The external loop at Line 6 parses each layer ℓ of \mathcal{G}' from the bottom layer 0 to the top layer L . At each iteration of the inner loop at Line 7,

³Parameter α might depend on n , e.g., the authors in [37] use $\alpha(n) = \log n$.

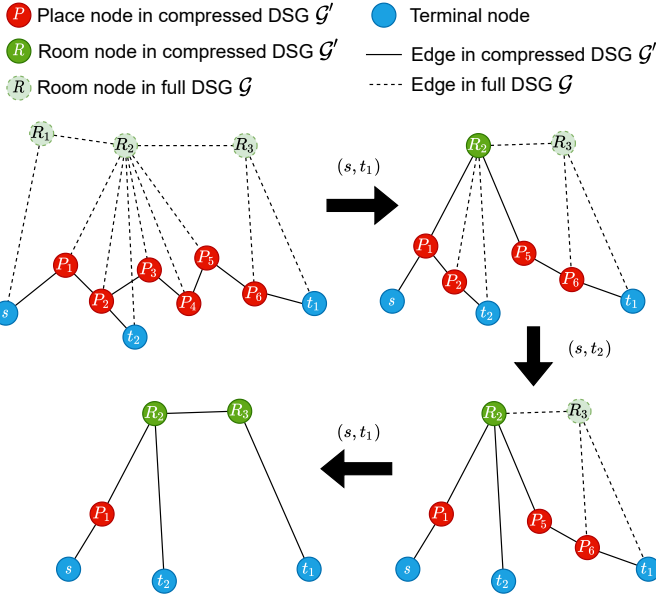


Figure 2: Illustration of the bottom-up compression procedure with one source s and two targets t_1 and t_2 . At each iteration, place nodes within a room are shortcut in the corresponding path. Nodes and edges are removed when neither of pairs (s, t_1) , (s, t_2) is connected through them. Note that the final graph cannot be further pruned without disconnecting terminals.

the algorithm checks if the shortest path $P_{G'}(s, t)$ connecting terminals s and t contains a stretch of consecutive nodes in layer $\ell - 1$, denoted by $\mathcal{V}_G(n_\ell)$ and named $(\ell - 1)$ -stretch, with the same parent node n_ℓ (Line 8): then, this node batch $\mathcal{V}_G(n_\ell)$ is removed from $P_{G'}(s, t)$ and replaced (compressed) with n_ℓ (Line 9).⁴ Importantly, such *compression* in the graph causes a corresponding *stretch* of the actual path followed by the robot, whose amount depends on both the interested layer ℓ and the amount of compressed nodes, in light of what discussed in Section IV-A. Nevertheless, the nested structure looping over layers externally (Line 6) and over paths internally (Line 7) introduces just one upper-layer abstraction at a time for each path (the layer ℓ is fixed in loop Line 7), and hence allows us to stretch distances in a balanced fashion, so that all paths are expected to suffer comparable distortion eventually. For example, if paths are made of place nodes, the first iteration of the inner loop compresses only one room for each path, so that at no point during the compression procedure a path is overcompressed w.r.t. other paths (for instance, it is not possible that a path is entirely abstracted to room nodes while another is kept with all place nodes). In general, this allows fine-scale spatial information to be retained as long as possible, and coarser layers (e.g., buildings) to be used only after finer layers (e.g., rooms) have been fully exploited for all paths (that is, building nodes can be used only if all paths contain room nodes and no place nodes). To ensure paths are always feasible,

⁴For consistency of navigation, we do not compress terminal nodes in our implementation, but this can be changed to meet communication constraints.

we use a data structure \mathcal{D} to track which paths are using nodes in G' : only when a node is traversed by no path (Line 13), it is removed from the graph.

Fig. 2 illustrates three consecutive iterations of Algorithm 2 on a toy DSG composed of place and room nodes. Dashed edges and light-colored nodes are part of the full (given) DSG G and potential candidates that can be added to the compressed representation G' , while the latter is marked with solid lines and dark node color. The spanner output by `build_spanner` at initialization contains only place nodes, thus retaining precise spatial information but not meeting the communication budget (top left). The first iteration of Algorithm 2 parses the shortest path from s to t_1 , abstracting away places in room R_2 (top right). Note that room R_1 is not considered because it does not provide budget reduction compared to keeping place P_1 . Also, place P_2 is not removed at this point because it is used to connect the other terminal pair. In fact, it is removed at the second iteration, when the shortest path from s to t_2 is entirely shortcut through place P_1 and room R_2 (bottom right). The final iteration removes place nodes in rooms R_2 and R_3 from the path connecting the first terminal pair, replacing those with the shortcut passing through room nodes (bottom left). An example on an actual DSG build from realistic synthetic navigation data is shown in Fig. 3: the initial spanner on the left is reduced to the compressed version on the right by exploiting the room node to abstract away several place nodes.

Algorithm 2 BUD-Lite

Input: DSG G , terminal pairs \mathcal{P} , communication budget B .
Output: Compressed DSG G' .

- 1: $G' \leftarrow \text{build_spanner}(G, \mathcal{P});$ // initialization
- 2: **for each** node $n \in \mathcal{V}_{G'}$ **do** // track node usage
- 3: $\mathcal{D}[n] = \{p_1^n, \dots, p_{m_n}^n\}$, where shortest path of each pair $p \in \{p_i^n\}_{i=1}^{m_n}$ in G' passes through node n ;
- 4: **end for**
- 5: **while** $|\mathcal{V}_{G'}| > B$ **do**
- 6: **for each** layer $\ell = 1, \dots, L$ **do**
- 7: **for each** $(s, t) \in \mathcal{P}$ **do** // parse path from s to t
- 8: **if** $\exists (\ell - 1)$ -stretch $\mathcal{V}_G(n_\ell) \subseteq P_{G'}(s, t)$ **then**
- 9: replace $\mathcal{V}_G(n_\ell)$ with parent n_ℓ in $P_{G'}(s, t)$;
- 10: $\mathcal{D}[n_\ell] \leftarrow \mathcal{D}[n_\ell] \cup (s, t)$;
- 11: **for each** node $n'_{\ell-1} \in \mathcal{V}_G(n_\ell)$ **do**
- 12: $\mathcal{D}[n'_{\ell-1}] \leftarrow \mathcal{D}[n'_{\ell-1}] \setminus (s, t)$;
- 13: **if** $\mathcal{D}[n'_{\ell-1}] = \emptyset$ **then** // if unused,
- 14: $G' \leftarrow G' \setminus \{n'_{\ell-1}\}$; // delete $n'_{\ell-1}$
- 15: **end if**
- 16: **end for**
- 17: **end if**
- 18: **end for**
- 19: **end while**
- 20: **return** G' .

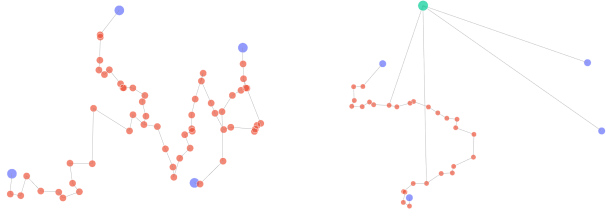


Figure 3: Initial (left) and final DSG spanners (right). Terminal nodes are in blue, place nodes in red, room node in green. DSG hierarchy-based compression sharply reduces graph size.

D. TOD-Lite: a Top-Down Expansion Algorithm

Symmetrically to the bottom-up approach of Algorithm 2, the idea behind Algorithm 3 (TOD-Lite, short for TOP-down D-Lite) is to exploit the DSG hierarchy top-down by expanding node children to iteratively increase spatial granularity of the compressed graph.

During initialization, Algorithm 3 first uses Algorithm 1 to build a spanner $\mathcal{G}'_{\text{target}}$ of the DSG, which is used as target for the final compressed graph \mathcal{G}' (Line 1). Then, it populates a "hierarchical spanner" \mathcal{H} (Line 2): this is simply a graph obtained from the original DSG \mathcal{G} by keeping only the spanner $\mathcal{G}'_{\text{target}}$ and nodes and edges encountered by climbing the DSG hierarchy starting from $\mathcal{G}'_{\text{target}}$ all the way to the top layer, while elements unrelated to the hierarchy of $\mathcal{G}'_{\text{target}}$ are removed. For example, if $\mathcal{G}'_{\text{target}}$ is made of place nodes, \mathcal{H} includes $\mathcal{G}'_{\text{target}}$, the room nodes associated with those places (together with edges among them), and possibly nodes above in the hierarchy, e.g., the buildings collecting those rooms. Graph \mathcal{H} is used to expand nodes from coarser to finer layers, as explained next. To define an expansion priority for nodes in the same layer, a data structure \mathcal{D} stores how many paths pass through each node in the graph, including both original paths in the target spanner (Line 4) and path abstractions in upper layers (Line 8): for example, the priority of a room node R is given by the number of paths actually passing through R in $\mathcal{G}'_{\text{target}}$ and of paths traversing place nodes associated with R .

The last phase is an iterative expansion through the hierarchical spanner \mathcal{H} . The output spanner \mathcal{G}' is initialized with terminal nodes (Line 11) and cross-layer connections (Line 12) to ensure minimum-cardinality paths, hence small communication cost.⁵ Then, starting from the top layer and one layer at a time (Line 17), each node in \mathcal{G}' is *expanded* if such operation does not exceed the budget (Lines 20 and 21), until no expansion is possible (Line 25). **In particular, if a node n_ℓ belonging to \mathcal{G}' has a set of children $\mathcal{V}_{\mathcal{H}}(n_\ell)$ in the hierarchical spanner \mathcal{H} , Line 20 adds to \mathcal{G}' nodes in $\mathcal{V}_{\mathcal{H}}(n_\ell)$ and Line 21 removes (*expands*) the parent n_ℓ . This mechanism is illustrated in Fig. 4, where room nodes R_1 , R_2 , and R_3 are progressively replaced with their children nodes. The starting condition (top left) ensures connectivity between terminals with low budget, but conveys little spatial information because of**

⁵Again, we assume that a minimal communication budget is always available to transmit at least such minimum-cost paths between terminals.

coarse abstractions.

Importantly, expanding nodes gradually restores the geometric granularity of the output spanner, because a spatially coarse representation (e.g., room node) is replaced by a group of nodes and edges carrying finer spatial resolution (e.g., in place layer). Such expansion of course comes at the price of heavier communication burden. Nonetheless, using the hierarchical spanner allows us to narrow the expansion procedure to a small set of navigation-relevant nodes, both saving runtime and helping meeting communication constraints.

Algorithm 3 TOD-Lite

Input: DSG \mathcal{G} , terminal pairs \mathcal{P} , communication budget B .

Output: Compressed DSG \mathcal{G}' .

```

1:  $\mathcal{G}'_{\text{target}} \leftarrow \text{build\_spanner}(\mathcal{G}, \mathcal{P})$ ;
2:  $\mathcal{H} \leftarrow \text{hierarchical spanner from } \mathcal{G}'_{\text{target}}$ ;
3: for each node  $n$  do // for node priority
4:    $\mathcal{D}[n] \leftarrow |\{p_1^n, \dots, p_{m_n}^n\}|$ , with shortest path of pair
    $p_i^n, i \in \{1, \dots, m_n\}$ , passing through node  $n$  in  $\mathcal{G}'_{\text{target}}$ ;
5: end for
6: for each layer  $\ell = L - 1, \dots, 0$  do
7:   for each node  $n_\ell$  do
8:      $\mathcal{D}[n_\ell] \leftarrow \mathcal{D}[n_\ell] \cup \bigcup_{n'_{\ell+1} \in \mathcal{V}_{\mathcal{G}}(n_\ell)} \mathcal{D}[n'_{\ell+1}]$ ;
9:   end for
10: end for
11:  $\mathcal{G}' \leftarrow \mathcal{P}$ ; // add terminals
12: for each  $(s, t) \in \mathcal{P}$  do // add cheapest path from  $s$  to  $t$ 
13:    $a \leftarrow$  lowest common ancestor of  $s$  and  $t$  in  $\mathcal{H}$ ;
14:    $\mathcal{G}' \leftarrow \mathcal{G}' \cup \{a\}$ ;
15:   connect  $s$  and  $t$  with  $a$  in  $\mathcal{G}'$ ;
16: end for
17: for each layer  $\ell = 0, \dots, L - 1$  do
18:   for each node  $n_\ell$  do // sorted by  $\mathcal{D}[n_\ell]$ 
19:     if expanding  $n_\ell$  does not exceed  $B$  then
20:        $\mathcal{G}' \leftarrow \mathcal{G}' \cup \mathcal{V}_{\mathcal{H}}(n_\ell) \cup \mathcal{E}_{\mathcal{H}}(\mathcal{V}_{\mathcal{H}}(n_\ell))$ ;
21:        $\mathcal{G}' \leftarrow \mathcal{G}' \setminus \{n_\ell\}$ ;
22:     end if
23:   end for
24:   if no node  $n_\ell$  has been expanded then
25:     break;
26:   end if
27: end for
28: return  $\mathcal{G}'$ .

```

Note that, with enough communication resources, this procedure would output exactly the target spanner $\mathcal{G}'_{\text{target}}$. Under limited budget, some nodes in $\mathcal{G}'_{\text{target}}$ cannot be expanded, e.g., a room may be used as a coarse representation of its places.

Comparison with [25]. Our nodal-expansion procedure resembles the approach used in [25]. However, there are fundamental differences between these two methodologies. First, we expand nodes along a preexisting semantic hierarchical structure (the 3D Scene Graph), while the hierarchy in [25] simply emerges from the regular geometry of the environment (such as grid map examples in [25, 46]), without awareness

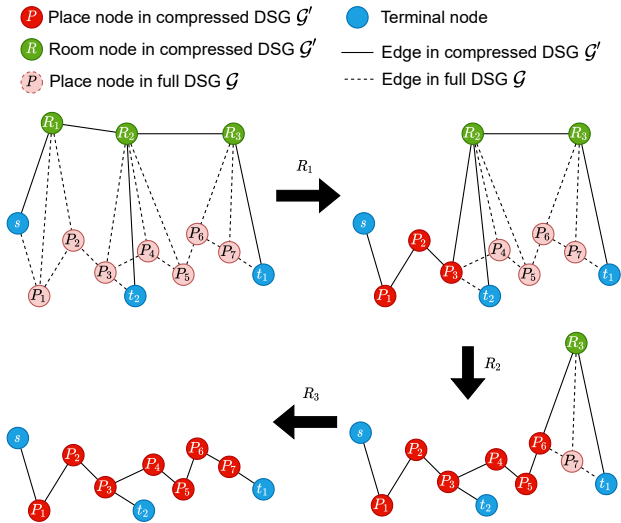


Figure 4: Illustration of the top-down expansion procedure with one source s and two targets t_1 and t_2 . At each iteration, a room node is expanded and replaced with its children place nodes. Adjacent place nodes are possibly added to ensure connectivity between terminals (e.g., P_3 at first iteration).

of semantics or physical quantities such as navigation time to move through coarse- and fine-scale maps. Second, our expansion leverages a target spanner computed up front and is guided by the navigation task, in particular by stretch introduced into shortest paths, while nodes in [25] are expanded based on an information-theoretic cost to be defined by suitable probability distributions whose support and density function change with expansions but are initially defined on the full graph to be compressed. More details about the algorithm in [25] are given in Section V

V. EXPERIMENTS

This section shows that the compressed DSG using our method is able to retain information for efficient navigation while meeting the bandwidth availability constraint. We also show that this can be done in real-time for online operation.

A. Experimental Setup

In addition to using the ILP exact formulation as a benchmark (since it does not scale with the size of the DSG), we also adapted the information theoretic abstraction approach proposed in [25] for comparison.

Q-Tree Search Adaptation. The graph abstraction framework proposed in [25] is based on the Information Bottleneck (IB) problem [47] to find the pruned representation T of the complete representation X by solving the relaxed version of the IB problem,

$$\min_{p(t|x)} I(T; X) - \beta I(T; Y), \quad (4)$$

where $I(T; X)$ is the mutual information between representations T and X and $I(T; Y)$ is the mutual information between

the pruned representation T and an additional random variable Y encoding relevant information about X . Parameter β then can be seen as the knob to adjust the amount of relevant information retained in T .

To adapt this framework to DSGs and for planning, we first define X by imposing a uniform distribution over the places in the DSG, next, we associate Y with the information of the shortest paths between terminal nodes and define $p(y_j|x_i) = 1$ if place x_i is on the shortest path y_j and $p(y_j|x_i) = 0$ otherwise. From the places layer, we propagate $p(x)$ and $p(y|x)$ to the rooms and buildings layers by a weighted sum as defined and shown in [25]. Additionally, we manually add the terminal nodes to the result if they are not automatically added by the algorithm, and in view of (1) the number of nodes is used as stopping condition in addition to the one presented in [25].

Simulator. We showcase the online operation of D-Lite in the uHumans2 simulator [48]. In the Office environment of the uHumans2 simulator, we devised four scenarios ranging from short, medium, to long in terms of the distance between the navigation goal and the starting position of the robot.

The queried robot r_2 sending the compressed DSG has no exact knowledge of the location of the querying robot r_1 , and is only given a number of potential locations. The places close to these terminal locations along with the place close to the navigation goal are the chosen as terminals for D-Lite. In the short and medium sequences, the source robot gets two putative locations, hence three total terminal nodes to account for when pruning. In the two long sequences, the source robot gets three putative locations, hence four total terminal nodes to account for when pruning. For all sequences we arbitrarily chose the budget to be 60 nodes, corresponding to about 1.6% of the full DSG.

Upon receiving the pruned DSG, the target robot r_1 immediately finds the place node s in the DSG closest to its current location, then computes the shortest path from s to the place node t that represents the navigation goal. The target then treats the nodes along the shortest path as waypoints to navigate to the goal. We combine the waypoint following with the use of the ROS navigation stack for local obstacle avoidance: the latter is needed when free-space locations (represented by places) are not made available to r_1 .

The complete results on the four scenarios are documented in Table I. We show the compression time (Comp), the nominal navigation time (Nom), the simulated mission time (Mis), and the size of the compressed DSG as averaged across three separate runs.

The nominal navigation time is computed by projecting the waypoints found onto the full DSG, calculating the total path length of traversing through the waypoints on the full DSG, and dividing by the maximum velocity of the agent in the simulator. In other words, it is the approximated optimal navigation time.

The combinatorial nature of the problem makes the exact (ILP) solver impractical for use in the real world. For the two longer runs, this approach was not able to find the compressed graph within an hour. The simulated mission time is faster for

Table I: Ablation table of results.

		Full	ILP	IB	BUD-Lite	TOD-Lite
short	Comp(s)	0	247	1	3	3
	Nom(s)	11	11	43	11	11
	Mis(s)	64	56	115	62	59
	Size(#)	3814	51	60	49	49
medium	Comp(s)	0	294	1	3	3
	Nom(s)	18	18	42	18	29
	Mis(s)	87	77	92	85	144
	Size(#)	3814	56	60	48	58
long1	Comp(s)	0	-	2	3	3
	Nom(s)	27	-	inf	31	39
	Mis(s)	134	-	inf	167	273
	Size(#)	3814	-	60	58	20
long2	Comp(s)	0	-	2	3	3
	Nom(s)	32	-	36	33	34
	Mis(s)	150	-	218	164	291
	Size(#)	3814	-	60	60	9

the compressed graph compared to the full DSG in some cases due to the former having to visit fewer waypoints, as having a sparser list of place node waypoints in a less cluttered space could actually lead to faster navigation.

In general, in all four sequences, the target robot is able to effectively reach the navigation goal using the pruned DSG output by D-Lite. The different performance of BUD-Lite (the bottom-up compression Algorithm 2) and TOD-Lite (the top-down expansion Algorithm 3) is due to the different pruning mechanisms, whereby the former performs better in most cases by virtue of finer node pruning. Note that discrepancies between nominal and simulated mission times are due to local navigation, whose exploration time is difficult to estimate *a posteriori*, but may be more reliably estimated by the robot while building the DSG online. Notably, our approaches always outperform IB as for both nominal and simulated mission time. Specifically, the compressed DSG generated by BUD-Lite yields navigation time that is within a minute of the optimal navigation time achieved by planning on the full DSG.

VI. CONCLUSIONS

Motivated by efficient navigation for robots that collaboratively explore an unknown environment, we have proposed algorithms to suitably compress 3D Scene Graphs built by robots during exploration when resource constraints of a shared communication channel make lossless transmission infeasible. Our algorithms can accommodate the presence of a sharp budget on the size of the transmitted map, run in real time, and perform graph compression with attention to the performance of queried navigation tasks. Simulated experiments carried out with a realistic simulator show that indeed our approach is able to meet sharp communication constraints while providing satisfactory performance of navigation tasks planned on the compressed DSG.

REFERENCES

[1] A. Rosinol, A. Gupta, M. Abate, J. Shi, and L. Carlone, "3D dynamic scene graphs: Actionable spatial perception with places, objects, and humans," in *Robotics: Science and Systems*

(RSS), 2020, (pdf), (media), (video). [Online]. Available: <http://news.mit.edu/2020/robots-spatial-perception-0715>

[2] N. Hughes, Y. Chang, and L. Carlone, "Hydra: a real-time spatial perception engine for 3D scene graph construction and optimization," in *Robotics: Science and Systems (RSS)*, 2022, (pdf).

[3] I. Armeni, Z. He, J. Gwak, A. Zamir, M. Fischer, J. Malik, and S. Savarese, "3D scene graph: A structure for unified semantics, 3D space, and camera," in *Intl. Conf. on Computer Vision (ICCV)*, 2019, pp. 5664–5673.

[4] S. Wu, J. Wald, K. Tateno, N. Navab, and F. Tombari, "SceneGraphFusion: Incremental 3D scene graph prediction from RGB-D sequences," in *IEEE Conf. on Computer Vision and Pattern Recognition (CVPR)*, 2021.

[5] A. Becker, P. N. Klein, and D. Saulpic, "A Quasi-Polynomial-Time Approximation Scheme for Vehicle Routing on Planar and Bounded-Genus Graphs," in *Proc. of the Annual European Symp. on Algorithms (ESA)*, vol. 87, 2017, pp. 12:1–12:15.

[6] A. C. Gilbert, T. Labs-Research, P. Avenue, F. Park, and K. Levchenko, "Compressing Network Graphs," *Proc. of the LinkKDD workshop at the ACM Conference on KDD*, vol. 124, p. 10, 2004.

[7] R. L. de Queiroz and P. A. Chou, "Compression of 3D Point Clouds Using a Region-Adaptive Hierarchical Transform," *IEEE Trans. on Image Processing*, vol. 25, no. 8, pp. 3947–3956, Aug. 2016.

[8] S. Raghavan and H. Garcia-Molina, "Representing Web graphs," in *Proc. International Conference on Data Engineering (Cat. No.03CH37405)*, Mar. 2003, pp. 405–416.

[9] C. Chekuri, T. Rukkanthant, and C. Xu, "On Element-Connectivity Preserving Graph Simplification," in *Algorithms - ESA 2015*, Berlin, Heidelberg, 2015, pp. 313–324.

[10] P. Harish, P. J. Narayanan, V. Vineet, and S. Patidar, "Chapter 7 - Fast Minimum Spanning Tree Computation," in *GPU Computing Gems Jade Edition*, ser. Applications of GPU Computing Series, Jan. 2012, pp. 77–88.

[11] K. Mehlhorn, "A faster approximation algorithm for the Steiner problem in graphs," *Information Processing Letters*, vol. 27, no. 3, pp. 125–128, Mar. 1988.

[12] R. Ahmed, G. Bodwin, F. D. Sahneh, K. Hamm, M. J. L. Jebelli, S. Kobourov, and R. Spence, "Graph spanners: A tutorial review," *Computer Science Review*, vol. 37, p. 100253, Aug. 2020.

[13] G. Bodwin, "On the Structure of Unique Shortest Paths in Graphs," in *Proc. of the Annual ACM-SIAM Symp. on Discrete Algorithms (SODA)*, Jan. 2019, pp. 2071–2089.

[14] M. Elkin and O. Neiman, "Efficient Algorithms for Constructing Very Sparse Spanners and Emulators," *ACM Trans. Algorithms*, vol. 15, no. 1, pp. 4:1–4:29, Nov. 2018.

[15] U. Kang and C. Faloutsos, "Beyond 'Caveman Communities': Hubs and Spokes for Graph Compression and Mining," in *Proc. of the IEEE International Conference on Data Mining*, Dec. 2011, pp. 300–309.

[16] M. Besta and T. Hoefler, "Survey and Taxonomy of Lossless Graph Compression and Space-Efficient Graph Representations," *arXiv:1806.01799 [cs, math]*, Apr. 2019.

[17] A. Borici and A. Thomo, "Semantic Graph Compression with Hypergraphs," in *IEEE International Conference on Advanced Information Networking and Applications*, Victoria, BC, Canada, May 2014, pp. 1097–1104.

[18] J.-G. Young, G. Petri, and T. P. Peixoto, "Hypergraph reconstruction from network data," *Commun. Phys.*, vol. 4, no. 1, p. 135, Dec. 2021.

[19] G. Karypis and V. Kumar, "Multilevel k-Way Hypergraph Partitioning," in *Design Automation Conference*, Jun. 1999, pp. 343–348.

[20] K. Devine, E. Boman, R. Heaphy, R. Bisseling, and U. Catalyurek, "Parallel hypergraph partitioning for scientific computing," in *Proc. of the IEEE International Parallel & Distributed Processing Symposium*, 2006, p. 10 pp.

[21] S. Zhang, Z. Ding, and S. Cui, "Introducing Hypergraph Signal Processing: Theoretical Foundation and Practical Applications," *IEEE Internet Things J.*, vol. 7, no. 1, pp. 639–660, Jan. 2020.

[22] T. Silver, R. Chitnis, A. Curtis, J. B. Tenenbaum, T. Lozano-Pérez, and L. P. Kaelbling, "Planning with Learned Object Importance in Large Problem Instances using Graph Neural Networks," *Proc. of the AAAI Conference on Artificial Intelligence*, vol. 35, no. 13, pp. 11 962–11 971, May 2021.

[23] C. Agia, K. M. Jatavallabhula, M. Khodeir, O. Miksik, V. Vineet, M. Mukadam, L. Paull, and F. Shkurti, "Taskography: Evaluating robot task planning over large 3D scene graphs," in *Conference on Robot Learning (CoRL)*. PMLR, Jan. 2022, pp. 46–58.

[24] Y. Tian, K. Khosoussi, and J. P. How, "A resource-aware approach

- to collaborative loop-closure detection with provable performance guarantees,” *Intl. J. of Robotics Research*, vol. 40, no. 10-11, pp. 1212–1233, Sep. 2021.
- [25] D. T. Larsson, D. Maity, and P. Tsiotras, “Q-Tree Search: An Information-Theoretic Approach Toward Hierarchical Abstractions for Agents With Computational Limitations,” *IEEE Trans. Robotics*, vol. 36, no. 6, pp. 1669–1685, Dec. 2020.
- [26] —, “Information-theoretic abstractions for resource-constrained agents via mixed-integer linear programming,” in *Proc. of the Workshop on Computation-Aware Algorithmic Design for Cyber-Physical Systems*, May 2021, pp. 1–6.
- [27] —, “A Generalized Information-Theoretic Framework for the Emergence of Hierarchical Abstractions in Resource-Limited Systems,” *Entropy*, vol. 24, no. 6, p. 809, Jun. 2022.
- [28] U. Kim, J. Park, T. Song, and J. Kim, “3-D scene graph: A sparse and semantic representation of physical environments for intelligent agents,” *IEEE Trans. Cybern.*, vol. PP, pp. 1–13, Aug. 2019.
- [29] R. Talak, S. Hu, L. Peng, and L. Carlone, “Neural trees for learning on graphs,” in *Conf. on Neural Information Processing Systems (NeurIPS)*, 2021, (pdf).
- [30] A. Dobson and K. E. Bekris, “Sparse roadmap spanners for asymptotically near-optimal motion planning,” *Intl. J. of Robotics Research*, vol. 33, no. 1, pp. 18–47, Jan. 2014.
- [31] P. N. Klein, “A subset spanner for Planar graphs, with application to subset TSP,” in *Proceedings of the Annual ACM Symposium on Theory of Computing*, ser. STOC ’06, May 2006, pp. 749–756.
- [32] I. Althöfer, G. Das, D. Dobkin, D. Joseph, and J. Soares, “On sparse spanners of weighted graphs,” *Discrete Comput Geom*, vol. 9, no. 1, pp. 81–100, Jan. 1993.
- [33] T. Kavitha, “New Pairwise Spanners,” in *International Symposium on Theoretical Aspects of Computer Science (STACS 2015)*, vol. 30, 2015, pp. 513–526.
- [34] S. Baswana, T. Kavitha, K. Mehlhorn, and S. Pettie, “Additive spanners and (a,b)-spanners,” *ACM Trans. Algorithms*, vol. 7, no. 1, pp. 5:1–5:26, Dec. 2010.
- [35] A. Abboud and G. Bodwin, “The $4/3$ Additive Spanner Exponent Is Tight,” *J. ACM*, vol. 64, no. 4, pp. 28:1–28:20, Sep. 2017.
- [36] M. Cygan, F. Grandoni, and T. Kavitha, “On Pairwise Spanners,” in *International Symposium on Theoretical Aspects of Computer Science (STACS)*, vol. 20, Dagstuhl, Germany, 2013, pp. 209–220.
- [37] M. Elkin, Y. Gitlitz, and O. Neiman, “Improved weighted additive spanners,” *Distrib. Comput.*, Aug. 2022.
- [38] —, “Almost Shortest Paths with Near-Additive Error in Weighted Graphs,” in *Proc. of the Scandinavian Symposium and Workshops on Algorithm Theory (SWAT)*, vol. 227, 2022, pp. 23:1–23:22.
- [39] R. Ahmed, G. Bodwin, F. D. Sahneh, S. Kobourov, and R. Spence, “Weighted Additive Spanners,” in *Graph-Theoretic Concepts in Computer Science*, ser. Lecture Notes in Computer Science, 2020, pp. 401–413.
- [40] R. Ahmed, G. Bodwin, F. D. Sahneh, K. Hamm, S. Kobourov, and R. Spence, “Multi-Level Weighted Additive Spanners,” in *Proc. of the International Symposium on Experimental Algorithms (SEA)*, vol. 190, 2021, pp. 16:1–16:23.
- [41] K. Censor-Hillel, T. Kavitha, A. Paz, and A. Yehudayoff, “Distributed construction of purely additive spanners,” *Distrib. Comput.*, vol. 31, no. 3, pp. 223–240, Jun. 2018.
- [42] S. Baswana and S. Sarkar, “Fully dynamic algorithm for graph spanners with poly-logarithmic update time,” in *Proc. of the Annual ACM-SIAM Symp. on Discrete Algorithms (SODA)*, Jan. 2008, pp. 1125–1134.
- [43] S. Arya, G. Dast, D. M. Mount, J. S. Salowe, and M. Smid, “Euclidean spanners: Short, thin, and lanky,” in *Proc. of the Acm Symposium on Theory of Computing*, 1995, pp. 489–498.
- [44] A. Abboud and G. Bodwin, “Reachability Preservers: New Extremal Bounds and Approximation Algorithms,” in *Proc. of the Annual ACM-SIAM Symp. on Discrete Algorithms (SODA)*, Jan. 2018, pp. 1865–1883.
- [45] Y. Kobayashi, “An FPT Algorithm for Minimum Additive Spanner Problem,” in *International Symposium on Theoretical Aspects of Computer Science (STACS)*, vol. 154, 2020, pp. 11:1–11:16.
- [46] D. T. Larsson, D. Maity, and P. Tsiotras, “Information-Theoretic Abstractions for Planning in Agents With Computational Constraints,” *IEEE Robotics and Automation Letters*, vol. 6, no. 4, pp. 7651–7658, Oct. 2021.
- [47] N. Tishby, F. Pereira, and W. Bialek, “The information bottleneck method,” *Proc. of the Allerton Conference on Communication, Control and Computation*, vol. 49, 07 2001.
- [48] A. Rosinol, A. Violette, M. Abate, N. Hughes, Y. Chang, J. Shi, A. Gupta, and L. Carlone, “Kimera: from SLAM to spatial perception with 3D dynamic scene graphs,” *Intl. J. of Robotics Research*, vol. 40, no. 12–14, pp. 1510–1546, 2021, arXiv preprint arXiv: 2101.06894, (pdf).

APPENDIX A
EXACT BUDGET-CONSTRAINED SPANNER

Problem (1) can be solved exactly by the following ILP (adapted from the exact spanner formulation in [40, Section 4]),

$$\min_{\substack{x_i \forall i \in \mathcal{V}_G \\ x_{i,j}^{st} \forall (i,j) \in \mathcal{E}_G, \forall (s,t) \in \mathcal{P}}} \beta \quad (5a)$$

$$\text{s.t.} \quad \sum_{(i,j) \in \bar{\mathcal{E}}_G} x_{(i,j)}^{uv} W^G(i,j) \leq d_G(s,t) + \beta W_{\max}^G(s,t) \quad \forall (s,t) \in \mathcal{P}, \forall (i,j) \in \mathcal{E}_G, \quad (5b)$$

$$\sum_{(i,j) \in \text{Out}(i)} x_{(i,j)}^{st} - \sum_{(j,i) \in \text{In}(i)} x_{(j,i)}^{st} = \begin{cases} 1 & i = s \\ -1 & i = t \\ 0 & \text{else} \end{cases} \quad \forall (s,t) \in \mathcal{P}, \forall i \in \mathcal{V}_G, \quad (5c)$$

$$\sum_{(i,j) \in \text{Out}(i)} x_{(i,j)}^{st} \leq 1 \quad \forall (s,t) \in \mathcal{P}, \forall i \in \mathcal{V}_G, \quad (5d)$$

$$x_i \geq x_{(i,j)}^{st} + x_{(j,i)}^{st} \quad \forall (s,t) \in \mathcal{P}, \forall i \in \mathcal{V}_G, \forall (i,j) \in \mathcal{E}_G, \quad (5e)$$

$$\sum_{i \in \mathcal{V}_G} x_i \leq B, \quad (5f)$$

$$x_i, x_{(i,j)}^{st} \in \{0, 1\} \quad \forall (s,t) \in \mathcal{P}, \forall i \in \mathcal{V}_G, \forall (i,j) \in \mathcal{E}_G, \quad (5g)$$

where x_i is associated with each node $i \in \mathcal{V}_G$ and is 1 if it is included in the spanner, $x_{(i,j)}^{st}$ is an edge variable equal to 1 if and only if edge (i,j) is taken as part of the path between s and t , $\bar{\mathcal{E}}_G$ is the augmented set of bidirected edges, obtained by adding edge (j,i) for each edge $(i,j) \in \mathcal{E}_G$, (5b) forces maximum distortion for all paths between terminal nodes, (5c)–(5d) ensure that the chosen edges form a path for each pair of terminals (s,t) , (5e) ensures that a node i is taken if any edges incident to it are taken, and (5f) encodes the limited budget on the number of selected nodes.

APPENDIX B
CALCULATION OF EDGE WEIGHTS

The edge weights associated with the intra-layer edges of the 3D Scene Graph \mathcal{G} are simply the Euclidean distance between the two nodes the edge connects. For example, for the layer consisting of places, the weight associated to an edge would be the Euclidean distance between the two connected places; for the layer consisting of rooms, the edge weight would be the Euclidean distance between the centroid of two rooms. The calculation of inter-layer edge weights is more nuanced: they cannot be simply Euclidean distances, since that would fail to capture the actual effort to traverse, for example, from a room to a place in the room. Instead, for inter-layer edges, we devise a method to associate to each edge a weight that is at least as large as the shortest path of traversal. For each inter-layer edge, we have a node in the higher level denoted as \mathbf{x} and a node in the lower level denoted as \mathbf{y} . To find the weight, we first find another node in the lower level \mathbf{y}_0 ; the weight of the edge $e_{\mathbf{x},\mathbf{y}}$ connecting \mathbf{x} and \mathbf{y} is then defined as

$$W^G(\mathbf{x}, \mathbf{y}) \doteq \|\mathbf{x} - \mathbf{y}_0\| + d_G(\mathbf{y}_0, \mathbf{y}) \quad (6)$$

where $\|\cdot\|$ denotes the Euclidean norm. Observe that the weight is greater than or equal to the path length of the shortest path between \mathbf{y}_0 and \mathbf{y} . Intuitively, the weight of a room-to-place inter-layer edge is the distance between the room centroid and the closest place, plus the path length from the closest place to the target place.